

Article

Effect of Heat Treatment Temperature on the Microstructure and Properties of Titanium-Clad Steel Plate Prepared by Vacuum Hot Rolling

Juan Pu ^{1,2,3,*} , Tingmu Chen ⁴, Yubo Sun ², Weimin Long ⁵, Huawei Sun ³ and Yunxia Chen ¹ 

¹ School of Intelligent Manufacturing and Control Engineering, Shanghai Polytechnic University, Shanghai 201209, China; cyx1978@yeah.net

² School of Materials Science and Engineering, Jiangsu University of Science and Technology, Zhenjiang 212003, China; suyub_513@163.com

³ China National Machinery Institute Group, Ningbo Intelligent Machine Tool Research Institute Co., Ltd., Ningbo 315700, China; windy314007@163.com

⁴ Fujian Special Equipment Inspection and Research Institute, National Quality Supervision and Inspection Center of Special Robot Product (Fujian), Quanzhou 362000, China; ctingmu@163.com

⁵ Zhengzhou Research Institute of Mechanical Engineering, Zhengzhou 450001, China; brazelong@163.com

* Correspondence: pu_juan84@163.com; Tel.: +86-15952815816

Abstract: Titanium-clad steel plates are widely used in chemical equipment and nuclear power equipment due to their excellent corrosion resistance and high strength. However, the Ti-C and Fe-Ti compounds generated easily at the titanium/steel interface deteriorate the bonding strength of titanium and steel, especially in high-temperature service environments. In this study, pure Fe DT4 was chosen as an intermediate layer to control the formation of interfacial compounds. The plates of titanium/DT4/steel were manufactured by hot rolling technology with a small hole vacuuming. Then, titanium-clad steel plates were annealed at temperatures of 450 °C, 550 °C, and 650 °C to modify microstructure and properties. The interfacial microstructure composition, mechanical properties of titanium-clad steel plates, and the corrosion resistance property of titanium plates were studied in the as-rolled state and under different annealing temperatures. The results showed that compounds of TiC, FeTi, and Fe₂Ti were generated at the interface of titanium-clad steel plates in the as-rolled state. After the annealing treatment, the types and quantities of the interfacial compounds were reduced, and these compounds were mainly TiC and FeTi at an annealing temperature of 450 °C. The interfacial compound was only TiC at an annealing temperature of 550 °C. However, the compounds of TiC and FeTi appeared at the interface at an annealing temperature of 650 °C. The variation of interfacial compounds determined the hardness and the shear strength of the titanium-clad steel plates. The more the interfacial compounds, the higher the hardness and the lower the shear strength. Therefore, when the annealing temperature was 550 °C, the interfacial hardness was lowest and the shear strength was highest. Meanwhile, the corrosion resistance of the titanium-clad plates showed significant improvement, indicating that this temperature provides favorable conditions for enhancing the corrosion performance of the plate.

Keywords: hot rolling technology with small hole vacuuming; titanium-clad steel plates; intermetallic compounds (IMCs); microstructure; corrosion resistance



Citation: Pu, J.; Chen, T.; Sun, Y.; Long, W.; Sun, H.; Chen, Y. Effect of Heat Treatment Temperature on the Microstructure and Properties of Titanium-Clad Steel Plate Prepared by Vacuum Hot Rolling. *Coatings* **2024**, *14*, 1096. <https://doi.org/10.3390/coatings14091096>

Academic Editor: Alina Vladescu

Received: 22 July 2024

Revised: 20 August 2024

Accepted: 26 August 2024

Published: 30 August 2024



Copyright: © 2024 by the authors. Licensee MDPI, Basel, Switzerland. This article is an open access article distributed under the terms and conditions of the Creative Commons Attribution (CC BY) license (<https://creativecommons.org/licenses/by/4.0/>).

1. Introduction

Titanium-clad steel plates are widely used in various fields such as petrochemical, marine engineering, and power plant desulfurization. As a result of the corrosion resistance of titanium alloys and the high strength and good plasticity of low-carbon steel especially, they can reduce the consumption of a single precious titanium alloy to save the cost [1–4].

Currently, there are three main methods to manufacture metal composite plates: explosive bonding, rolling, and explosive + rolling. During the process of explosive bonding and

explosive + rolling bonding, the stability of the explosive bonding is decreased with the plate area increasing. If the plate area is too large, mismatch occurs and poor bonds appear at the edges of the composite plate and the product yield rate is low. Additionally, the environmental pollution problems caused by explosions, such as shock waves, noise, and dust, become increasingly serious as the number of explosives increases proportionally [5,6]. Hot rolling technology does not have the above problem of explosive bonding, but the surface of the billet is prone to oxidizing during the high-temperature heating process, which affects the interface bonding of the metal composite plates. To solve the oxidation at high temperatures, JFE corporation in Japan was the first to integrate vacuum electron beam welding with hot rolling to form the relatively mature technology of vacuum rolling. Meanwhile, small hole vacuuming can also be used to produce billets with the help of a mechanical pump to extract the air inside the billets. Vacuum hot rolling can produce thin laminated metal composite plates with a width exceeding 3000 mm. Compared with the vacuum electron beam rolling, the hot rolling technology with small hole vacuuming is simpler and its production cost is lower [7,8], thus it is used in small and medium-sized enterprises.

There are some differences in the physical and chemical properties between titanium and steel. Therefore, even if hot rolling with small hole vacuuming is used to prepare titanium-clad steel plates, there are still some problems. On the one hand, the deformation of two substrates is inconsistent during the hot rolling process. On the other hand, intermetallic compounds (IMCs) such as TiC, FeTi, and Fe₂Ti are easily formed at the interface of titanium-clad steel plates. These brittle IMCs are prone to becoming stress concentration points and crack propagation sources. This will deteriorate the interfacial bonding strength of the titanium/steel [9–11].

Scholars have reported a lot about the IMCs' formation in titanium-clad steel plates [12–14]. Jiang et al. [15], Chu et al. [16], and so on confirmed that IMCs such as FeTi, Fe₂Ti, and TiC generate at the interface of TA1 titanium and Q235 steel. To control the formation of interfacial IMCs, Yan et al. [17] selected Ni as an intermediate layer to inhibit the formation of TiC and TiFe compounds between titanium and stainless steel during hot rolling. Moreover, Ni reacted with Ti to generate TiNi, TiNi₃, and Ti₂Ni compounds so that the bonding strength of the titanium and stainless steel was improved. Li et al. [18] believed that using Cu as an intermediate layer could suppress the mutual diffusion of elements Fe and Ti, thereby reducing the generation of brittle IMCs at the interface. However, the grain size of interfacial IMCs increased and the interfacial shear strength decreased after the titanium-clad steel plates annealing. Chai et al. [19] found that intermediate layers of Nb and Mo can effectively reduce the generation of TiC and Fe₂Ti compounds, but micropores appeared at the interface of the titanium-clad steel plates. The size and quantity of these micropores were related to the shear strength of the titanium-clad steel. The shear strength can reach a value of 290 MPa when using Nb as the intermediate layer with the small size of the micropores. However, the shear strength decreased a lot when using Mo as the intermediate layer with the large size micropores. Although these intermediate layer materials mentioned above can improve the interfacial bonding strength of titanium-clad steel, their cost is high. Several studies have shown that choosing pure Fe as the intermediate layer can decrease production costs greatly. Yu et al. [20] manufactured titanium-clad steel plates with pure iron DT4 as the intermediate layer in vacuum hot rolling technology. The results showed that the interfacial shear strength reached up to a maximum of 237.6 MPa with the rolling temperature of 850 °C. It seemed that adding an intermediate layer can reduce the number of interfacial IMCs and improve the bonding strength of titanium-clad steel plates; moreover, pure iron was considered the most economical material among these intermediate layer materials.

After the vacuum hot rolling of titanium-clad steel plates, the plates were annealed to eliminate the residual stress and improve their plasticity and toughness. The annealing temperature and holding time had a significant impact on the properties of the titanium-clad steel plates. Li et al. [21] reported that titanium and steel were rolling bonded using interstitial free (IF) steel and vanadium (V) as interlayers, and then the as-rolled clad plates

were subjected to different post-rolling annealing treatments. The shear strength and the tensile strength of the annealed clad plates decreased with the increase in holding time and annealing temperature. Reductions in the strength were mainly attributed to the co-existence of the σ phase and vanadium carbides. Jiang et al. [22] annealed the titanium-clad steel plates for about 60 min at temperatures of 650 °C, 750 °C, 850 °C, and 950 °C. The microstructure of the samples underwent recovery and recrystallization during the annealing process, and the shear strength decreased quickly once the temperature was over 850 °C. Wang et al. [23] used explosive + rolling technology to prepare the titanium-clad steel plates with DT4 pure iron as the intermediate layer first and then the as-rolled plates were annealed at temperatures from 550 °C to 1000 °C. He pointed out that the interfacial shear strength reached its maximum with temperatures ranging from 550 °C to 650 °C. The above research indicates that the interfacial bonding of clad plates is optimal when the annealing temperature is no more than 650 °C.

Therefore, TA2 titanium and Q235B steel were hot rolled by using small hole vacuuming with DT4 pure iron as the intermediate layer in this paper. Then, the as-rolled clad plates were annealed with a holding time of 2 h at temperatures of 450 °C, 550 °C, and 650 °C. The microstructure, shear strength, and corrosion resistance of the clad plates in the as-rolled state and under different annealing temperatures was systematically studied. The evolution mechanism of the IMCs at the interface of the clad plates was explored. The relationship of the annealing temperature with the interfacial microstructure, the shear strength, and the corrosion resistance of the clad plates was established.

2. Experimental Materials and Methods

TA2 titanium with a size of 11.5 mm × 1500 mm × 2200 mm and Q235B steel with a size of 80 mm × 1600 mm × 2300 mm were selected as the clad metals. DT4 pure iron with a thickness of 1 mm was used as the intermediate layer to control the formation of brittle IMCs at the interface. Their chemical compositions and properties are listed in Tables 1 and 2.

Table 1. Chemical composition of the clad metals (wt. %).

Elements	C	Si	Mn	Fe	N	H	Ti	O	Al	S	P
TA2	0.030	-	-	0.300	0.009	0.002	Bal.	0.25	-	-	-
Q235B	0.2	0.2	0.2	Bal.	-	-	-	-	-	0.03	0.03
DT4	0.148	0.15	0.6	Bal.	-	-	-	-	0.023	0.003	0.017

Table 2. Physical and mechanical properties of the clad metals.

Materials	Density (g/cm ³)	Thermal Conductivity W/(m·K)	Coefficient of Linear Expansion (10 ⁻⁶ ·K ⁻¹)	Melting Points (°C)	Tensile Strength (MPa)	Elongation after Fracture A (%)
TA2	4.51	21.9	8.6	1668	441	20
Q235B	7.85	49.8	12	1468	487	30

Titanium-clad steel plates were manufactured by hot-rolling technology with small hole vacuuming. Its rolling process is shown in Figure 1. Firstly, a symmetrical structure of Q235B steel/DT4 pure iron/TA2 titanium/Barrier agent/TA2 titanium/DT4 pure iron/Q235B steel was equipped to improve the production efficiency and prevent the deformation of the plates during rolling. Wherein, a barrier agent with a thickness of approximately 0.3 mm~0.4 mm was coated on the interface of the two TA2 titanium to prevent adhesion during hot rolling. The barrier agent was a mixture of magnesium oxide, water glass, and polyvinyl alcohol. Secondly, assembled samples were sealed and were joined around the plates by submerged arc welding. Then, samples were vacuumed with a small hole and the vacuum degree reached up to a value of 5 Pa. Finally, the process of multi-layer combined rolling was conducted. The billet was heated to 880 °C in a resistance

furnace and held for 4 h, and then rolled 16 times at a temperature of 850 ± 10 °C. The overall compression rate was up to the value of 90%, and the titanium-clad steel plates with a thickness of 10 mm for steel and 1.2 mm for titanium were completed. The as-rolled titanium-clad steel plates were annealed at temperatures of 450 °C, 550 °C, and 650 °C, respectively, with the same holding time of 2 h.

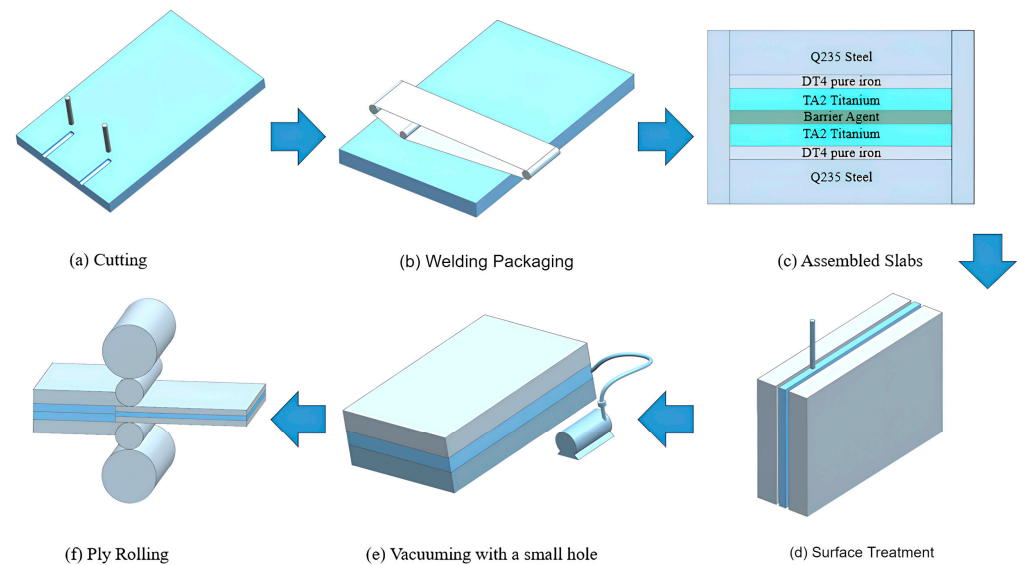


Figure 1. Manufacturing process flow of titanium-clad steel plates.

Titanium-clad steel plates were ground with sandpapers, polished with SiO_2 suspension, then corroded by using a solution including hydrofluoric acid, nitric acid, and deionized water with a volume ratio of 2:1:50 for the titanium side and by using a 4% nitric acid solution for the steel side. The interfaces of titanium-clad steel plates were observed by using a ZEISS optical microscope (OM, Jena, Germany) and a JSM-6480 scanning electron microscope (SEM, JEOL, Tokyo, Japan). The characteristic points and the element distribution at the interface were analyzed by using energy dispersive spectroscopy (EDS, Carl Zeiss, Jena, Germany) and mapping scanning. A titanium-clad steel plate was peeled off along its interface, and the phase analysis on the surface of TA2 titanium and Q235B steel was performed by using an X-ray diffractometer (XRD-6000, Shimadzu, Kyoto, Japan). The process parameters were a scanning rate of $6^\circ/\text{min}$, a step width of 0.02° , and an angle of $10^\circ\sim 90^\circ$. The morphologies were observed using transmission electron microscopy (TEM, JEM-2100F, JEOL, Tokyo, Japan). Samples were first sliced into discs with a thickness of 0.25 mm with a diamond saw. These discs were mechanically ground and then thinned by using a double-jet electropolisher with an electrolyte of 90% perchloric acid and 10% ethyl alcohol at -30 °C and 20 mA. Bright-field images and selected area electron diffraction (SAED) patterns of interfacial compounds were obtained.

The tensile and shear tests on the titanium-clad steel plates were performed by GB/T8547-2006 «Titanium-clad steel plates» and GB/T6369-2008 «Test Methods for Mechanical and Process Properties of Composite Steel Plates». The sizes of the samples are shown in Figure 2. The tensile and shear tests were conducted on a CMT5205 electronic universal testing machine, with a tensile and shear rate of 1 mm/min. The final results were derived from the average of the four samples. The microhardness at the interface of titanium-clad steel plates was tested by KB30s automatic Vickers hardness tester with a load of 100 g.

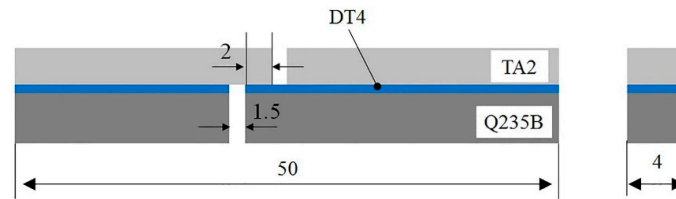


Figure 2. Schematic diagram of the tension-shear sample.

The corrosion resistance of the titanium-clad plate was tested by using the EG M283 electrochemical workstation with a three-electrode system. The titanium layer served as the working electrode, the reference electrode was used as a saturated calomel electrode, and the auxiliary electrode was used as a platinum electrode. The polarization curve and AC impedance spectrum of the sample were tested in 10% H₂SO₄ solution. The parameters were set as follows: EIS measurements were performed in the frequency range between 10 mHz and 100 KHz, an AC sine wave amplitude of 10 mV, and for potentiodynamic polarization measurements the scanning rate was 1 mV/s and potential range was $-1.5\sim 1.5$ V.

3. Results and Discussion

3.1. Microstructure Analysis of Titanium-Clad Steel Plates

Figure 3 shows the morphology of as-rolled and annealed titanium-clad steel plates with DT4 pure iron as the intermediate layer. From Figure 3a, it can be seen that the plates included three zones of Q235B steel, a pure iron transition zone, and TA2 titanium. The microstructure of the steel was mainly composed of striped ferrite and pearlite. The width of the pure iron transition zone was about 120 μm . The microstructure of TA2 exhibited a hot-rolled state. The interface between TA2 and DT4 was relatively straight and smooth. Some black inclusions and some micropores appeared occasionally, but no microcrack and non-fusion existed at the interface. This indicated that using pure iron as the intermediate layer can achieve effective metallurgical bonding between TA2 and Q235B.

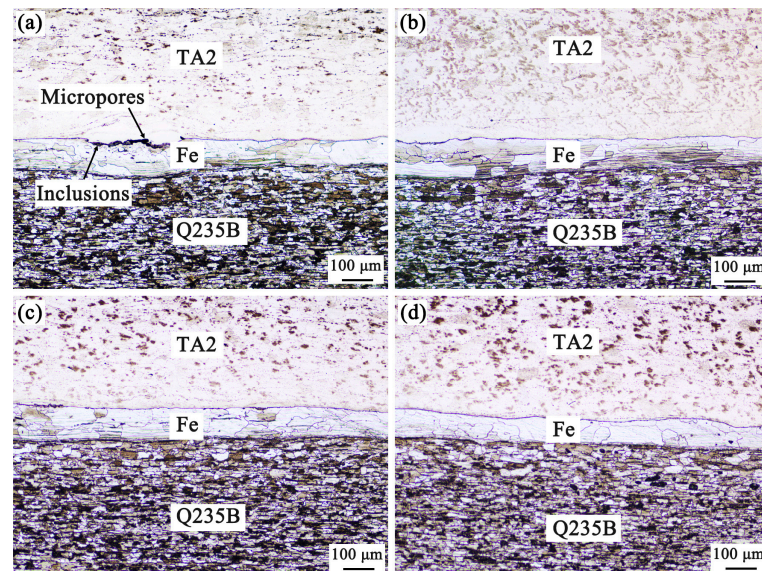


Figure 3. Interfacial morphologies of titanium-clad steel plates under different annealing temperatures: (a) as-rolled; (b) 450 °C; (c) 550 °C; (d) 650 °C.

After annealing at the temperatures of 450 °C, 550 °C, and 650 °C, shown in Figure 3b–d, respectively, elements at both sides of the interface diffused more fully, thus the number of micropores and black inclusions at the interface reduced, which was beneficial to improving the bonding strength of the interface. Compared with the as-rolled titanium-clad steel plates, the grain size and the width of the pure iron transition zone of the samples after annealing

decreased slightly. Moreover, the width of the transition zone decreased gradually with the increase in annealing temperatures.

To analyze the effect of different annealing temperatures on the diffusion behavior of elements Fe, C, and Ti at the interface of the samples, SEM line scanning analysis on the interfaces was performed, and the results are shown in Figure 4. For the as-rolled samples, as shown in Figure 4a, the element Ti diffused from TA2 to the Ti/Fe interface and ended at a distance of 0.6 μm along the pure iron transition zone. The element Fe diffused from the pure iron transition zone towards the TA2 side, and the Fe content reached its minimum at a distance of 0.3 μm along the Ti/Fe interface. The content of element C didn't change much at the Ti/Fe interface, which indicated that the addition of a pure iron layer hindered the diffusion of element C from the Q235 steel side to the TA2 titanium alloy side.

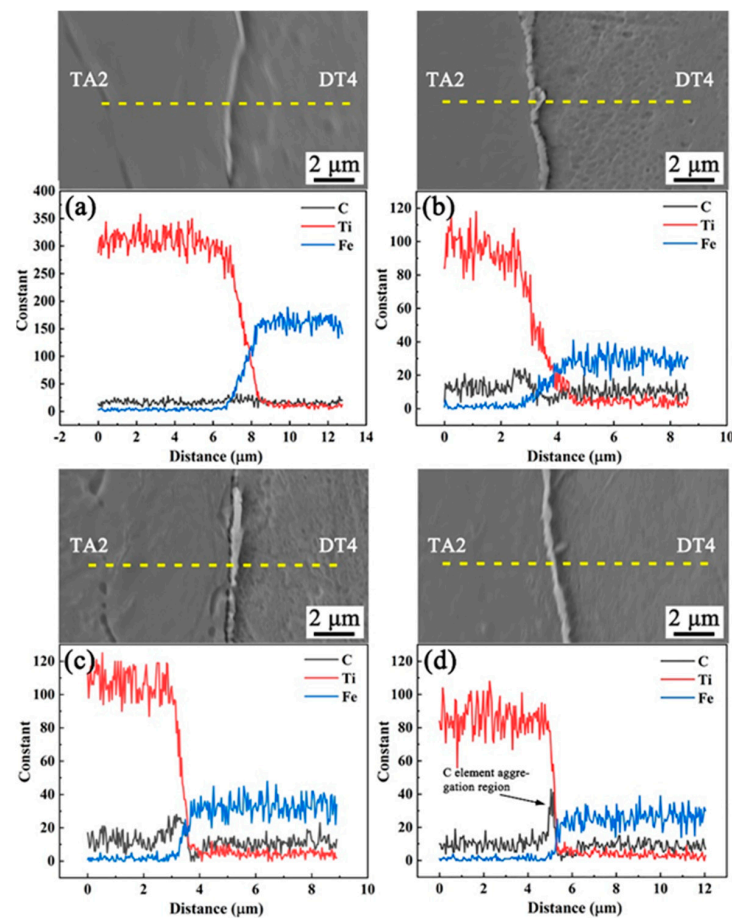


Figure 4. Elements distribution profiles of the interface between TA2 and DT4 under different annealing temperatures: (a) as-rolled; (b) 450 °C; (c) 550 °C; (d) 650 °C.

After annealing, the elements Fe, Ti, and C on both sides of the Ti/Fe interface diffused completely, and thus the peak content of these elements decreased. The curve on the distribution of elements Ti and Fe did not vary much but the element C changed a lot under annealing temperatures of 450 °C, 550 °C, and 650 °C. From Figure 4b,c, a large amount of element C diffused towards the side of TA2. Element C gathered at a distance of 1 μm away from the interface of Ti/Fe. It can be inferred that TiC compounds are generated on the TA2 side. With the increase in annealing temperature, elements Fe and Ti became saturated and element C gathered at the interface near the TA2 side, as shown in Figure 4d.

Figure 5 shows the SEM surface analysis results of element distribution at the interface of Ti/Fe under different annealing temperatures. Element C distribution on both sides of Ti/Fe changed with the annealing temperature increasing. For the as-rolled sample, element C was uniformly distributed in the TA2 and DT4, without aggregation at the

interface of TA2/DT4, as shown in Figure 5a. This phenomenon was attributed to the fact that the addition of pure iron DT4 slowed the diffusion of element C from Q235 to TA2 partly and reduced the generation of carbides at the Ti/Fe interface. After annealing treatment, the content of element C distributing in the samples increased obviously but the content of elements Ti and Fe decreased; meanwhile, element C diffused from Q235 steel through the pure iron DT4 to the TA2 titanium and gathered at the interface near the side of TA2 titanium. When the annealing temperature was 550 °C, element C gathered at the interface to form a clear line, as shown in Figure 5b,c. From Figure 5d, when the annealing temperature was increased to 650 °C, the carbon layer thickness at the interface increased. It indicated that when the samples were annealed at temperatures of 450 °C~650 °C, it was beneficial for element C to diffuse, which was prone to aggregate at the interface of TA2/DT4 so that the diffusion of elements Ti and Fe was hindered and the contents of the Fe-Ti compounds was reduced. However, the excessive diffusion of element C may lead to the formation of amounts of carbides near the interface, thereby reducing the bonding strength of TA2 and DT4.

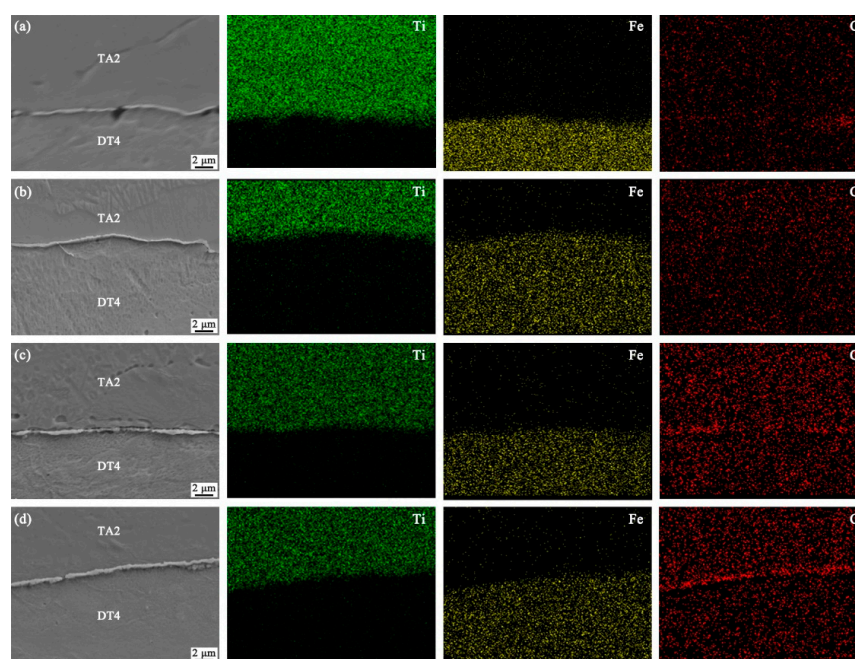


Figure 5. Element distribution of interface between TA2 titanium alloy and DT4 pure iron under different annealing temperatures: (a) as-rolled; (b) 450 °C; (c) 550 °C; (d) 650 °C.

To analyze the interfacial phase composition of titanium-clad steel plates, XRD phase analysis was performed on both sides of TA2 and DT4, as shown in Figure 6. From Figure 6, TiC and FeTi compounds formed at the side of TA2, while TiC, FeTi, and Fe₂Ti compounds formed at the side of DT4 for the as-rolled sample. After annealing the samples, the phase composition at the Ti/Fe interface changed with the increase in annealing temperatures. When the temperature was 450 °C, TiC compounds formed at the side of TA2 and FeTi compounds formed at the side of DT4. Once the temperature was increased to 550 °C, only TiC compounds formed at the interface of Ti/Fe. However, when the temperature was 650 °C, TiC compounds were generated at the side of TA2 and FeTi compounds formed at the side of DT4.

Figure 7 lists the TEM results of the interface between TA2 and DT4 in the as-rolled state. The results confirmed that the compounds of FeTi, Fe₂Ti, and TiC formed at the interface. In the process of ply rolling with a small hole to pump vacuum, symmetrical assembled slabs can solve the incompatibility of the plates' deformation which resulted from the large difference in yield strength and elongation between titanium and steel.

However, no matter how to adjust the rolling process and post-treatment process, the brittle IMCs of TiC, FeTi, and Fe₂Ti formed inevitably due to the inter-diffusion of elements C, Ti, and Fe at the interface. These brittle compounds will deteriorate the mechanical properties of the samples. Adding a pure Fe interlayer can prolong the diffusing path of elements Fe, Ti, and C thus reducing the formation of brittle IMCs at the interface.

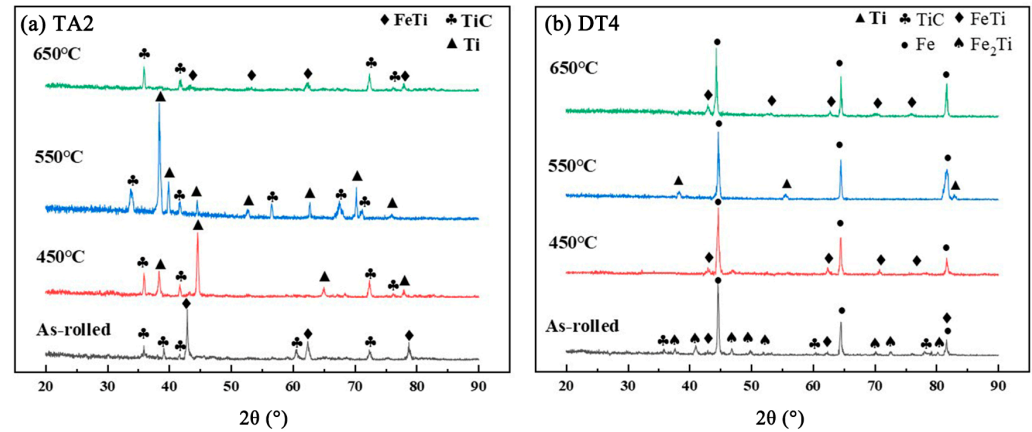


Figure 6. XRD results of samples: (a) TA2 side; (b) DT4 side.

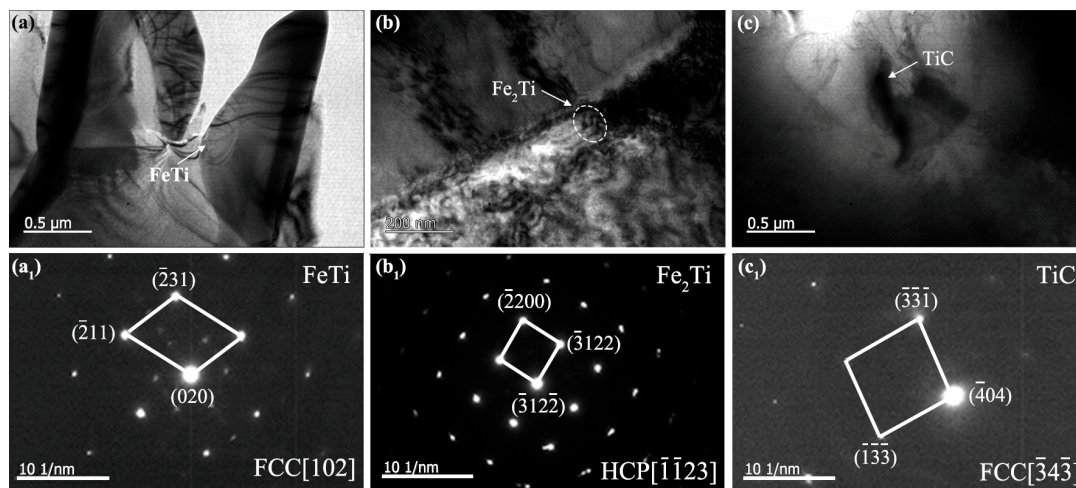


Figure 7. TEM results of the interface between TA2 and DT4 in the as-rolled state: (a,a₁) FeTi; (b,b₁) Fe₂Ti; and (c,c₁) TiC.

Figure 8 displays the schematic diagram of element diffusion at the interface under different annealing temperatures. In the as-rolled state, TiC and Fe-Ti compounds formed at the interface, but the distribution of these compounds were not uniform, as shown in Figure 8a. With the increase in annealing temperature, the mutual diffusion rate among Fe, Ti, and C elements improved, which promoted the bonding of the titanium and steel [24]. From a thermodynamic perspective, the order of standard Gibbs free energy of these compounds is TiC < FeTi < Fe₂Ti < 0 [25], which indicates that a TiC compound forms optimally at the interface. Meanwhile, the diffusion coefficient of C element is relatively high and the content of C element in TA2 is low, which resulted in a concentration difference of C element on both sides of the interface. During the annealing process, C element diffused rapidly from the steel side into the interface, and a small amount of Fe and Ti elements diffused towards the interface. Therefore, when the annealing temperature was 450 °C, the TiC compound formed preferentially at the location with a higher C element concentration and the FeTi compound also formed locally at the interface, as shown in Figure 8b. When the annealing temperature was 550 °C, the C element aggregated continuously with the

annealing time prolonging and then a TiC compound layer formed at the interface. The TiC compound layer acts as a barrier to hinder the diffusion of Fe element towards the interface, thereby suppressing the formation of brittle Fe-Ti compounds, as shown in Figure 8c. However, when the annealing temperature was 650 °C, Fe-Ti compounds began to precipitate at the interface after depleting carbon due to carbon's strong affinity with titanium, as shown in Figure 8d.

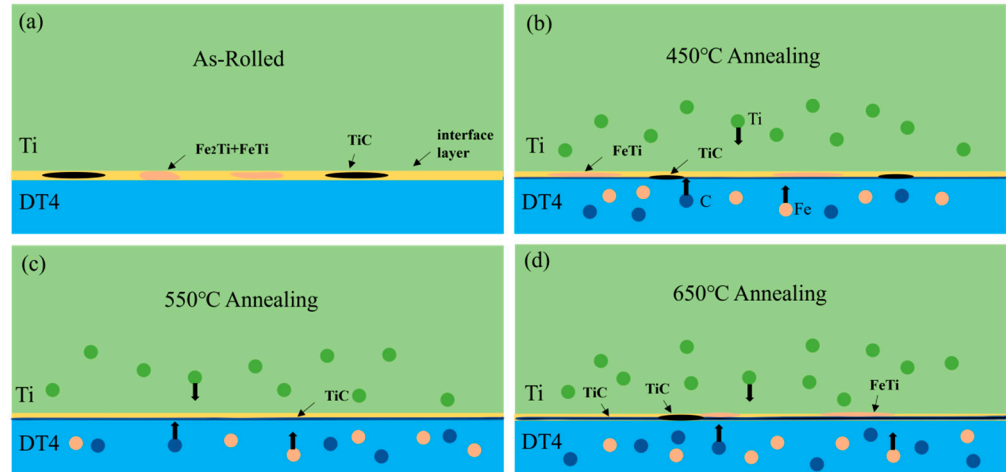


Figure 8. Schematic diagram of elements diffusion at the interface under different annealing temperatures: (a) as-rolled; (b) 450 °C; (c) 550 °C; (d) 650 °C.

3.2. Microhardness Analysis of Titanium-Clad Steel Plates

Figure 9 shows the microhardness variation curves of samples in the as-rolled state and after annealing treatment. It can be concluded that the microhardness of titanium-clad steel reached up to the maximum at the interface whether in the as-rolled state or the annealing state. In the as-rolled state, the microhardness at the interface reached a value of 370 HV as a result of compounds of FeTi, Fe₂Ti, and TiC. After annealing at temperatures of 450 °C~650 °C, the microhardness decreased because the interfacial microstructure was refined. When the annealing temperature increased from 450 °C to 550 °C, the interfacial microhardness decreased from 280 HV to 230 HV. This was mainly attributed to compounds changing from TiC and FeTi to TiC. When the annealing temperature was 650 °C, the microhardness was 246 HV with the interfacial compound of FeTi and TiC.

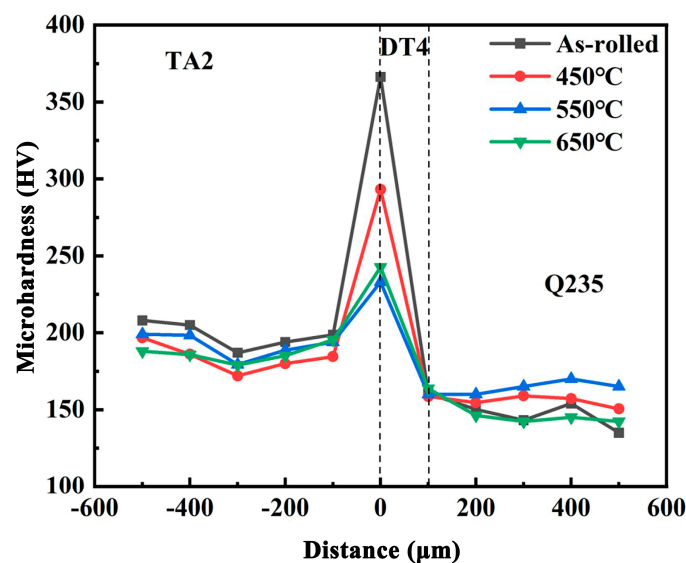


Figure 9. Microhardness variation curve of titanium-clad steel plates.

3.3. Analysis of the Shear Strength of Titanium-Clad Steel Plates

Figure 10 reflects the shear resistance of samples in an as-rolled state and under different annealing temperatures. The shear strength of the sample in the as-rolled state was 184.5 MPa. After the annealing treatment, its shear strength increased first and then decreased a little. When the annealing temperature was 550 °C, its shear strength reached up to a maximum of 195.4 MPa. The interface bonding strength of the titanium-clad steel plates was related to the diffusion of elements and the types of compounds at the interface. During the as-rolled state, compounds of FeTi and Fe₂Ti appeared at the interface of the samples, which decreased its shear strength. After annealing, element C reacted with element Ti to form TiC, which hindered the mutual diffusion of elements Fe and Ti to some extent. Especially, only TiC appeared at the interface of the samples at an annealing temperature of 550 °C, thus its shear strength reached up to the maximum. However, when the annealing temperature increased to 650 °C, element Ti started to react with element Fe to form compounds of FeTi at the interface of the samples; these brittle compounds decreased the shear strength of the samples. Therefore, the shear strength of the samples depended on the number and type of compounds at the interface; compounds of FeTi, Fe₂Ti, and TiC coexisted at the interface, and the shear strength of the samples got worse.

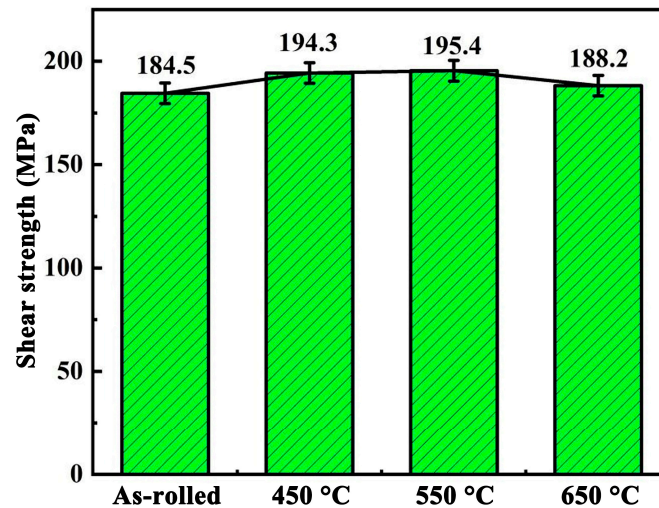


Figure 10. Effect of the annealing temperature on the shear strength of titanium-clad steel plates.

The samples fractured at the interface Ti/Fe during the shear test process. Figure 11 shows the shear fracture morphology of samples in an as-rolled state and under different annealing temperatures. These fracture morphologies exhibited typical brittle fractures. The size of the cleavage steps in the as-rolled state reached the maximum while the size of the cleavage steps with an annealing temperature of 550 °C was up to the minimum. The size of the cleavage steps was related to the shear strength of the samples. The smaller the size of the cleavage steps, the better the shear strength of the samples. This was consistent with the variation trend of the shear strength of the samples.

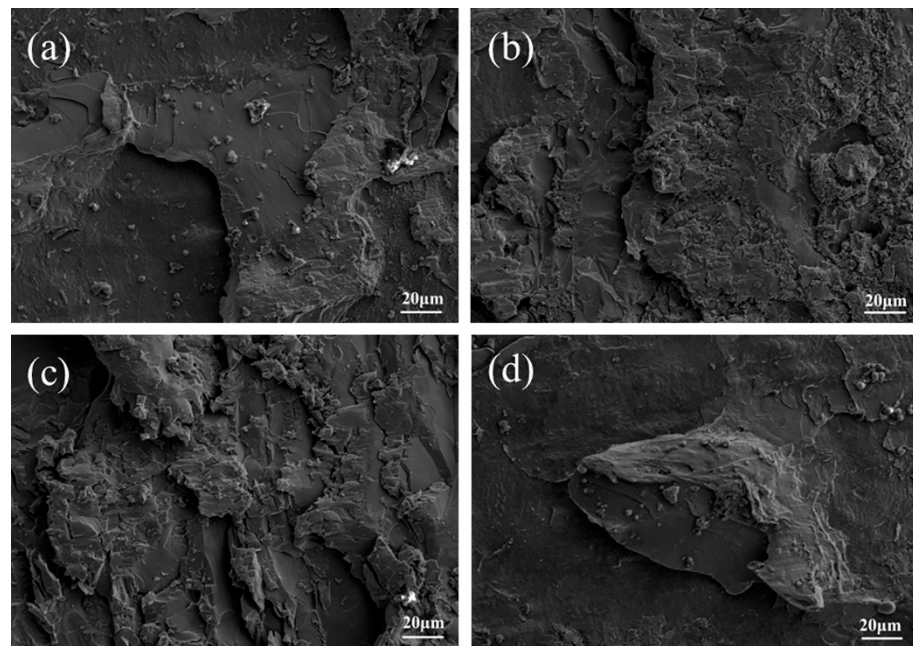


Figure 11. Shear fracture morphology of titanium-clad steel plates under different annealing temperatures: (a) as-rolled; (b) 450 °C; (c) 550 °C; (d) 650 °C.

3.4. Corrosion Resistance Analysis on TA2 Titanium Plates

The sample was peeled off and then electrochemical corrosion testing on the TA2 titanium plate in a 10 % H_2SO_4 solution was conducted. Figure 12 shows the polarization curves of TA2 titanium alloy plates in the as-rolled state and under different annealing temperatures. It can be seen from the curve that a passivation zone (0.25 V~1.75 V) appeared for all the samples, and the current density changed a bit with the potential increase in the passivation zone. This indicated that sample surfaces were in a passive state during the corrosion process. The peak potential in the passivation zone was the breakdown potential [26]. When the potential exceeded 1.75 V, the passivation film began to rupture, then the sample underwent pitting corrosion, and finally the corrosion rate of the samples increased sharply. In a comparison of the samples in as-rolled and annealing states, the breakdown potential of the sample was approximately 1.5 V in the as-rolled state. After the annealing treatment, the breakdown potential was approximately between 1.6 V and 1.75 V. When the annealing temperature increased from 450 °C to 650 °C, the breakdown potential first increased and then decreased slightly and it was up to the maximum with the annealing temperature of 550 °C. This means that the passivation film of this sample maintained a stable state for the longest time and had the best corrosion resistance performance.

The polarization curve was fitted by using Cview2 software and the fitted self-corrosion potential and corrosion current density are listed in Table 3. The corrosion current density reflects the actual corrosion rate of the samples and the lower the corrosion current density, the smaller the corrosion rate [27–29]. From Table 3, the self-corrosion potential of the samples obeyed the following relationship: 550 °C (0.573 V) > 450 °C (−0.575 V) > 650 °C (−0.587 V) > as-rolled state (−0.654 V), while the corrosion current density was 550 °C (3.614×10^{-5}) < 450 °C (4.020×10^{-5}) < 650 °C (4.264×10^{-5}) < as-rolled state (4.546×10^{-5}). It demonstrated that the corrosion resistance property of the TA2 titanium alloy plate was optimal under an annealing temperature of 550 °C.

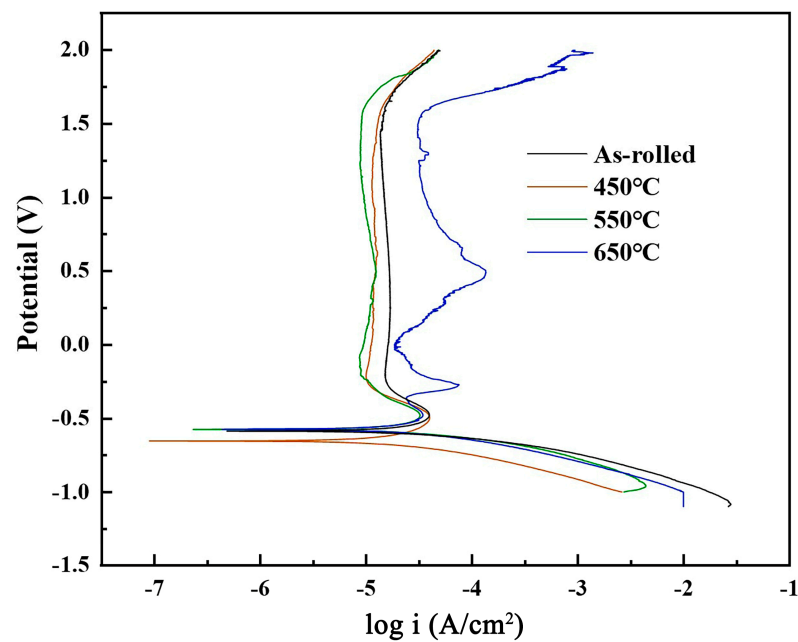


Figure 12. Dynamic potential polarization curves of TA2 titanium plates under different annealing temperatures.

Table 3. The fitting results of the polarization curve shown in Figure 10 used by Cview software.

Temperature (°C)	E_{corr} (mV)	I_{corr} ($\text{A} \cdot \text{cm}^2$)
As-rolled	−0.654	4.546×10^{-5}
450	−0.575	4.020×10^{-5}
550	−0.573	3.614×10^{-5}
650	−0.587	4.264×10^{-5}

To investigate the stability of the passivation film, Electrochemical Impedance Spectroscopy (EIS) testing for the passivation film was performed. The sample was placed in a 10 % H_2SO_4 solution and passivated at a constant potential of 0.2 V vs. SCE for 2 h to ensure the preparation of a stable passivation film on the surface of the sample. EIS results are shown in Figure 13. Figure 13a presents the Nyquist curve, which consists of a high-frequency capacitor circuit and a low-frequency inductor circuit. The radius of the capacitor circuit is used to characterize corrosion resistance [30–32]. The larger the radius of the capacitor circuit, the more stable the passivation film and the better the corrosion resistance of the samples. The order of the capacitive arc radius in the Figure 13a was $R_{550^\circ\text{C}} > R_{450^\circ\text{C}} > R_{650^\circ\text{C}} > R_{\text{As-rolled}}$. Thus, TA2 titanium-clad plate annealed at a temperature of 550 °C had the largest capacitance arc radius and the best stability of the passivation film.

Figure 13b shows the relationship among Bode- $|Z|$, Bode-phase angle, and frequency. In general, the higher the $|Z|$ value, the better the corrosion resistance property in the low-frequency range. When the annealing temperature was 550 °C, the $|Z|$ value was the highest and its corresponding corrosion resistance in the low-frequency range of the sample was best. Moreover, the larger the phase angle in the Bode diagram, the more uniform the current distribution and the lower the corrosion rate [33]. All phase angles were greater than 45 ° in Figure 13, which indicated that the current distribution in the samples was uniform and the corrosion performance was good. TA2 titanium-clad plate had the highest phase angle and the best corrosion resistance property under an annealing temperature of 550 °C.

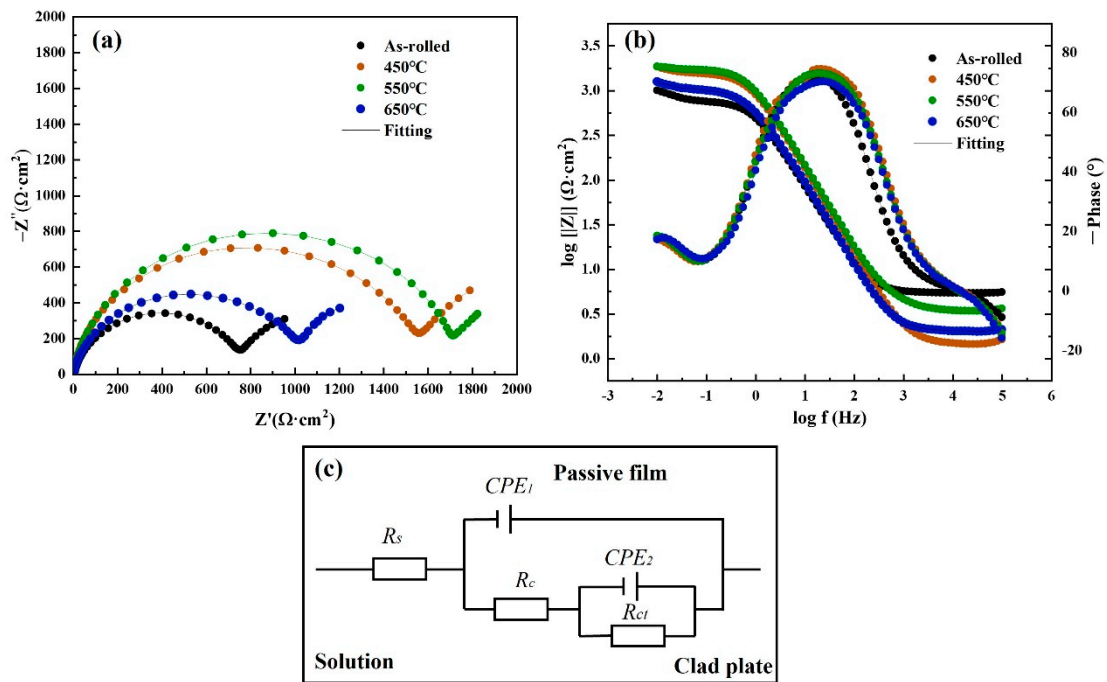


Figure 13. Electrochemical Impedance Spectroscopy (EIS) of TA2 titanium alloy plate: (a) Nyquist plots; (b) Bode plots; (c) Fitting circuit diagram.

Figure 13c presents the equivalent circuit, which is used to fit the impedance data of passive film. In this model, R_s represents the solution resistance, R_{ct} is the charge transfer resistance of the passive film, R_c is the internal impedance of the TA2 titanium-clad plate, and CPE is the constant phase angle element. Table 4 lists the electrochemical fitting parameters based on the equivalent circuit displayed in Figure 13c. Both R_c and R_{ct} increased at first and then decreased with the increase in the annealing temperature. When the annealing temperature was 550 °C, the maximums of R_c and R_{ct} were 1770 $\Omega \cdot \text{cm}^2$ and 2356 $\Omega \cdot \text{cm}^2$, respectively, which suggested that the compactness and stability of the passive film was optimal.

Table 4. Fitting parameters of EIS results obtained from a proposed equivalent mode.

Temperature (°C)	R_s ($\Omega \cdot \text{cm}^2$)	$CPE_1 \times 10^{-4}$ ($\Omega^{-1} \text{cm}^{-2} \text{S}^{-n}$)	n_1	R_c ($\Omega \cdot \text{cm}^2$)	$CPE_2 \times 10^{-2}$ ($\Omega^{-1} \text{cm}^{-2} \text{S}^{-n}$)	n_2	R_{ct} ($\Omega \cdot \text{cm}^2$)	$\chi^2 \times 10^{-4}$
As-rolled	5.385	2.66	0.914	767.7	2.79	0.927	758.7	3.18
450	1.492	1.48	0.943	1535	1.74	0.807	2112	6.32
550	3.529	1.50	0.918	1770	4.30	0.986	2356	1.95
650	2.017	0.23	0.923	1047	1.89	0.781	1762	7.70

4. Conclusions

Titanium-clad steel plates were prepared by a hot rolling technology with a small hole vacuuming and using pure Fe as the intermediate layer. Then, plates were annealed at temperatures of 450 °C, 550 °C, and 650 °C. The interfacial microstructure composition and mechanical properties of the titanium-clad steel plates, as well as the corrosion resistance of the titanium-clad plates in the as-rolled state and under different annealing temperatures, were studied. The main results are as follows:

(1) When choosing pure Fe as the intermediate layer, whether in the as-rolled state or annealed at temperatures of 450 °C~650 °C, titanium-clad steel plates were excellent. After annealing treatment, elements at the interface of titanium and steel diffused more completely.

(2) In the as-rolled state, the interfacial compounds of the samples consisted of TiC, FeTi, and Fe₂Ti. After annealing at a temperature of 450 °C, these interfacial compounds changed into TiC and FeTi. However, when the annealing temperature was 550 °C, only the compound TiC was generated at the interface. When the annealing temperature increased to 650 °C, compounds TiC and FeTi appeared again at the interface.

(3) In the as-rolled state, the interface microhardness of Ti/Fe was the highest. When the annealing temperature increased from 450 °C to 650 °C, its microhardness first decreased and then increased slightly, and it reached a minimum annealing temperature of 550 °C.

(4) Annealing treatment promoted the diffusion of elements at the interface of Ti/Fe. As the annealing temperature was 550 °C, the compound TiC was generated at the interface which hindered the formation of brittle phases between Fe and Ti. The varieties and quantities of the interface compounds were few. The shear strength of the titanium-clad steel plates rose to a maximum of 195.4 MPa, and the corrosion resistance of the titanium-clad plate was optimal.

Author Contributions: Conceptualization, J.P. and H.S.; methodology, Y.S.; Investigation, J.P. and Y.S.; validation, T.C., W.L. and H.S.; writing—original draft preparation, J.P.; writing—review and editing, Y.S., W.L. and Y.C.; supervision, T.C., W.L., H.S. and Y.C. All authors have read and agreed to the published version of the manuscript.

Funding: This research was supported by Shanghai Polytechnic University (No. C80ZK230037, No. C80ZK240037, No. C80ZK242003, No. C80ZK242002), by Jiangsu University (High-tech Ship) Cooperative Innovation Centre and Institute of Marine Equipment, Jiangsu University of Science and Technology (No. HZ2018008), and Jiangsu Province Undergraduate Innovation Project and Jiangsu Key Laboratory Project of Green Ship Technology (No. 2019Z02).

Institutional Review Board Statement: Not applicable.

Informed Consent Statement: Not applicable.

Data Availability Statement: The data presented in this study are available on request from the corresponding author due to scientific research.

Conflicts of Interest: The author Juan Pu is conducting her postdoctoral research at the Ningbo Intelligent Machine Tool Research Institute Co., Ltd., Huawei Sun was employed by Ningbo Intelligent Machine Tool Research Institute Co., Ltd. The remaining authors declare that the research was conducted in the absence of any commercial or financial relationships that could be construed as a potential conflict of interest.

References

1. Su, H.; Luo, X.B.; Chai, F.; Shen, J.C.; Sun, X.J.; Lu, F. Manufacturing Technology and Application Trends of Titanium Clad Steel Plates. *J. Iron Steel Res. Int.* **2015**, *22*, 977–982. [[CrossRef](#)]
2. Kundu, S.; Sam, S.; Chatterjee, S. Interface microstructure and strength properties of Ti–6Al–4V and microduplex stainless steel diffusion bonded joints. *Mater. Des.* **2011**, *32*, 2997–3003. [[CrossRef](#)]
3. Jiang, H.T.; Yan, X.Q.; Liu, J.X.; Zeng, S.W.; Duan, X.G. Diffusion Behavior and Mathematical Model of Ti-Steel Explosive Clad Plate during Heat Treatment. *Rare Met. Mater. Eng.* **2015**, *44*, 972–976.
4. Zu, G.Y.; Sun, X.; Zhang, J.H. Interfacial Bonding Mechanism and Mechanical Performance of Ti/Steel Bimetallic Clad Sheet Produced by Explosive Welding and Annealing. *Rare Met. Mater. Eng.* **2017**, *46*, 906–911.
5. Jiang, C.; Long, W.M.; Feng, J.; Zhang, L.; Zhang, S. Interfacial microstructure and mechanical properties of copper/stainless steel fabricated by explosive welding. *Weld. Join.* **2021**, *09*, 22–27.
6. Sun, J.F.; Liang, X.J.; Jiao, S.H. Study on the interface of direct hot rolling titanium-clad steel plates. *Baosteel Tech. Res.* **2017**, *11*, 32–39.
7. Bai, Y.L.; Liu, X.F.; Wang, W.J.; Yang, Y.H. Current status and research trends in processing and application of titanium/steel composite plate. *Chin. J. Eng.* **2021**, *43*, 85–96.
8. Yu, C.; Fu, L.; Xiao, H.; Lv, Q.; Gao, B.X. Effect of carbon content on the microstructure and bonding properties of hot-rolling pure titanium clad carbon steel plates. *Mater. Sci. End. A* **2021**, *820*, 141572. [[CrossRef](#)]
9. Chai, X.Y.; Shi, Z.R.; Chai, F.; Su, H.; Yang, Z.G.; Yang, C.F. Effect of Heating Temperature on Microstructure and Mechanical Properties of Titanium Clad Steel by Hot Roll Bonding. *Rare Met. Mater. Eng.* **2019**, *48*, 2701–2710.

10. Wang, G.L.; Luo, Z.A.; Xie, G.M.; Wang, L.P.; Zhao, K. Effect of heating temperature on the bonding property of the Titanium/Stainless Steel Plate by Hot-Rolling Bonding. *Rare Met. Mater. Eng.* **2013**, *42*, 387–391.
11. Luo, Z.A.; Xie, G.M.; Wang, G.L.; Wang, G.D. Effect of interfacial Microstructure on Mechanical Properties of Vacuum Rolling Clad Pure Titanium/High Strength Low Alloy Steel. *Chin. J. Mater. Res.* **2013**, *27*, 569–575.
12. Gloc, M.; Wachowski, M.; Plocinski, T.; Kurzydowski, K.J. Microstructural and microanalysis investigations of bond titanium grade1/low alloy steel st52-3N obtained by explosive welding. *J. Alloys Compd.* **2016**, *671*, 446–451. [[CrossRef](#)]
13. Yang, D.H.; Luo, Z.A.; Xie, G.M.; Jiang, T.; Zhao, S.; Misra, R.D.K. Interfacial microstructure and properties of a vacuum roll-cladding titanium-steel clad plate with a nickel interlayer. *Mater. Sci. Eng. A* **2019**, *753*, 49–58. [[CrossRef](#)]
14. Luo, Z.A.; Wang, G.L.; Xie, G.M.; Wang, L.P.; Zhao, K. Interfacial microstructure and properties of a vacuum hot roll-bonded Titanium-Stainless Steel Clad Plate with a Niobium Interlayer. *Acta Metall. Sin. Engl. Lett.* **2013**, *26*, 754–760. [[CrossRef](#)]
15. Jiang, C.; Long, W.M.; Zhong, S.J.; Fan, X.G.; Liao, Z.Q.; Wei, Y.Q. Interface microstructure and properties of TA1/Q235R explosive welding clad plate. *Electr. Weld. Mach.* **2023**, *53*, 65–70.
16. Chu, Q.L.; Zhang, M.; Li, J.H.; Yan, C. Experimental and numerical investigation of microstructure and mechanical behavior of titanium/steel interfaces prepared by explosive welding. *Mater. Sci. Eng. A* **2017**, *689*, 323–331. [[CrossRef](#)]
17. Yan, J.C.; Zhao, D.S.; Wang, C.W.; Wang, L.Y.; Wang, Y.; Yang, S.Q. Vacuum hot roll bonding of titanium alloy and stainless steel using nickel interlayer. *Mater. Sci. Technol.* **2013**, *25*, 914–918. [[CrossRef](#)]
18. Li, X.B.; Li, X.H.; Li, M.; Zhang, S.; Jiang, Q.W. Effect of annealing on element diffusion of TA1/Q235 clad sheet. *Trans. Mater. Heat Treat.* **2017**, *38*, 35–40.
19. Chai, X.Y.; Pan, T.; Chai, F.; Luo, X.B.; Su, H.; Yang, Z.G.; Yang, C.F. Interlayer engineering for titanium clad steel by hot roll bonding. *J. Iron Steel Res. Int.* **2018**, *25*, 739–745. [[CrossRef](#)]
20. Yu, C.; Xiao, H.; Yu, H.; Qi, Z.C.; Xu, C. Mechanical properties and interfacial structure of hot-roll bonding TA2/Q235B plate using DT4 interlayer—ScienceDirect. *Mater. Sci. Eng. A* **2017**, *695*, 120–125. [[CrossRef](#)]
21. Li, B.X.; He, W.J.; Chen, Z.J.; Mo, T.Q.; Peng, L.; Li, J.; Liu, Q. Influence of annealing on the microstructure, interfacial compounds and mechanical properties of hot rolling bonded Ti/steel clad plate with bimetallic interlayered steel and vanadium. *Mater. Sci. Eng. A* **2019**, *764*, 138221–138227. [[CrossRef](#)]
22. Jiang, H.T.; Yan, X.Q.; Liu, J.X.; Duan, X.G. Effect of heat treatment on microstructure and mechanical property of Ti-Steel explosive-rolling clad plate. *Trans. Nonferrous Met. Soc. China* **2014**, *24*, 697–704. [[CrossRef](#)]
23. Wang, J.Z.; Yan, X.B.; Wang, W.Q.; Yan, J.Y.; Rong, Y.; Yan, P. Titanium cladding steel plates with interlayer by explosion and rolling bonding. *Rare Met. Mater. Eng.* **2010**, *39*, 309–313.
24. Zhao, G.H.; Tang, Q.Y.; Guo, Q.C.; Li, J.; Ma, L.F.; Ma, L.W. Effect of annealing temperature on interfacial microstructure and tensile fracture behavior of titanium-steel clad plate. *Mater. Charact.* **2024**, *215*, 114128. [[CrossRef](#)]
25. Bai, Y.L.; Liu, X.F. Interfacial reaction behavior of titanium/steel composite plate formed by cold-hot rolling. *Mater. Charact.* **2023**, *202*, 113030. [[CrossRef](#)]
26. Meng, K.; Guo, K.; Yu, Q.; Miao, D.; Yao, C.; Wang, Q.F.; Wang, T.S. Effect of annealing temperature on the microstructure and corrosion behavior of Ti-6Al-3Nb-2Zr-1Mo alloy in hydrochloric acid solution. *Corros. Sci.* **2021**, *183*, 109320. [[CrossRef](#)]
27. Zhang, Y.F.; Yuan, X.G.; Huang, H.J.; Zuo, X.J.; Cheng, Y.L. Influence of chloride ion concentration and temperature on the corrosion of Cu–Al composite plates in salt fog. *J. Alloys Compd.* **2020**, *821*, 153249. [[CrossRef](#)]
28. Zhang, C.; Wu, M.F.; Pu, J.; Shan, Q.; Sun, Y.B.; Wang, S.Q.; Hermann, S.K.U.G. Effect of Cu Coating on Microstructure and Properties of Al/Steel Welding–Brazing Joints Obtained by Cold Metal Transfer (CMT). *Coatings* **2022**, *12*, 1123. [[CrossRef](#)]
29. Pu, J.; Xie, P.; Long, W.M.; Wu, M.F.; Sheng, Y.W.; Sheng, J. Effect of current on corrosion resistance of duplex stainless steel layer obtained by plasma arc cladding. *Crystals* **2022**, *12*, 341. [[CrossRef](#)]
30. Meenakshi, K.S.; Kumar, S.A. Corrosion resistant behaviour of titanium–Molybdenum alloy in sulphuric acid environment. *Mater. Today Proc.* **2022**, *65*, 3282–3287. [[CrossRef](#)]
31. Mao, T.; Li, L.; Huang, H.B.; Yu, Z.M.; Zhong, Y.; Chen, S.L. Corrosion behaviors of TA2 and TA36 titanium alloys in a high-sulfur environment. *Int. J. Electrochem. Sci.* **2024**, *19*, 100462.
32. Liu, H.D.; Pu, J.; Wu, M.F.; Zhang, C.; Rao, J.W.; Long, W.M.; Shen, Y.X. Research on the Microstructure and Properties of Al Alloy/Steel CMT Welding–Brazing Joints with Al–Si Flux-Cored. *Coatings* **2023**, *13*, 1590. [[CrossRef](#)]
33. Wei, Y.; Pan, Z.M.; Fu, Y.; Yu, W.; He, S.L.; Yuan, Q.Y.; Luo, H.; Li, X.G. Effect of annealing temperatures on microstructural evolution and corrosion behavior of Ti–Mo titanium alloy in hydrochloric acid. *Corros. Sci.* **2022**, *197*, 110079. [[CrossRef](#)]

Disclaimer/Publisher’s Note: The statements, opinions and data contained in all publications are solely those of the individual author(s) and contributor(s) and not of MDPI and/or the editor(s). MDPI and/or the editor(s) disclaim responsibility for any injury to people or property resulting from any ideas, methods, instructions or products referred to in the content.